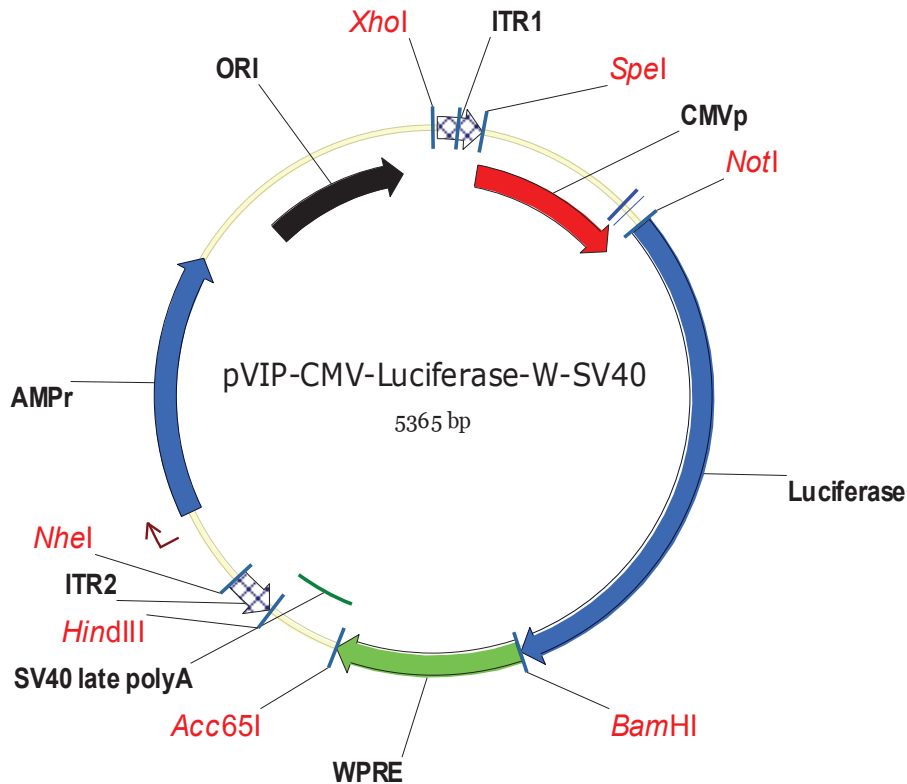


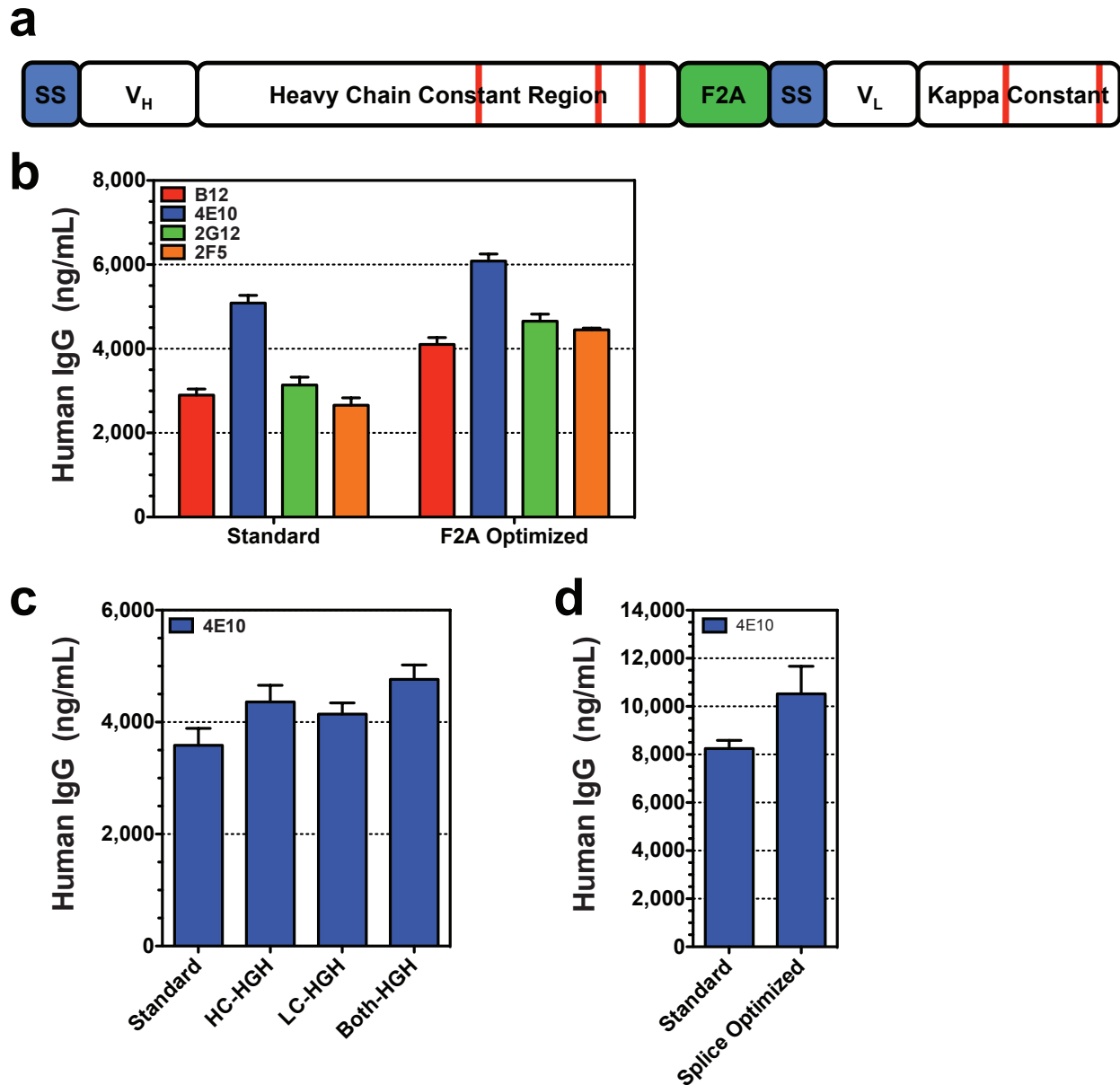
Supplementary Figure 1 – Development of a muscle-optimized AAV-based antibody expression vector

a, (left) Quantitation of luciferase activity by Xenogen imaging of $\text{Rag2}^{-/-}\gamma\text{c}^{-/-}$ mice receiving intramuscular injection of 1×10^{10} or 1×10^{11} GC of AAV2/8 encoding luciferase demonstrates long-term dose-dependent expression ($n=2$). (right) Concentration of human IgG in circulation as measured by total human IgG ELISA on serum samples taken after intramuscular injection of 1×10^{10} or 1×10^{11} GC of AAV2/8 expressing 4E10-IgG1 into $\text{Rag2}^{-/-}\gamma\text{c}^{-/-}$ mice ($n=2$). Antibody production is dose-dependent and is maintained for at least 64 weeks. **b**, Comparison of luciferase activity 15 weeks after intramuscular injection of 2×10^9 GC of AAV2/8 vectors expressing luciferase from a panel of promoters ($n=2$). **c**, Design of the CASI promoter combining the CMV enhancer and chicken β -actin promoter followed by a splice donor (SD) and splice acceptor (SA) flanking the ubiquitin enhancer region. **d**, Comparison of luciferase activity from vectors driven by CASI as compared to conventional promoters 8 weeks after intramuscular injection of 1×10^9 GC of AAV2/8 encoding luciferase driven by the indicated promoter ($n=2$). **e**, Comparison of luciferase activity 6 weeks post-administration of CMV-driven vectors with or without WPRE, terminated by the indicated polyadenylation signal ($n=2$). **f**, Schematic representation of the VIP expression vector for antibody expression indicating the inverted terminal repeats (ITR), the CASI promoter, an IgG1 heavy chain linked to kappa light chain separated by a self-processing 2A sequence, a WPRE for improved expression and SV40 late-polyadenylation signal. Antibody V-regions of heavy and light chains are cloned into the vector at positions indicated in red.



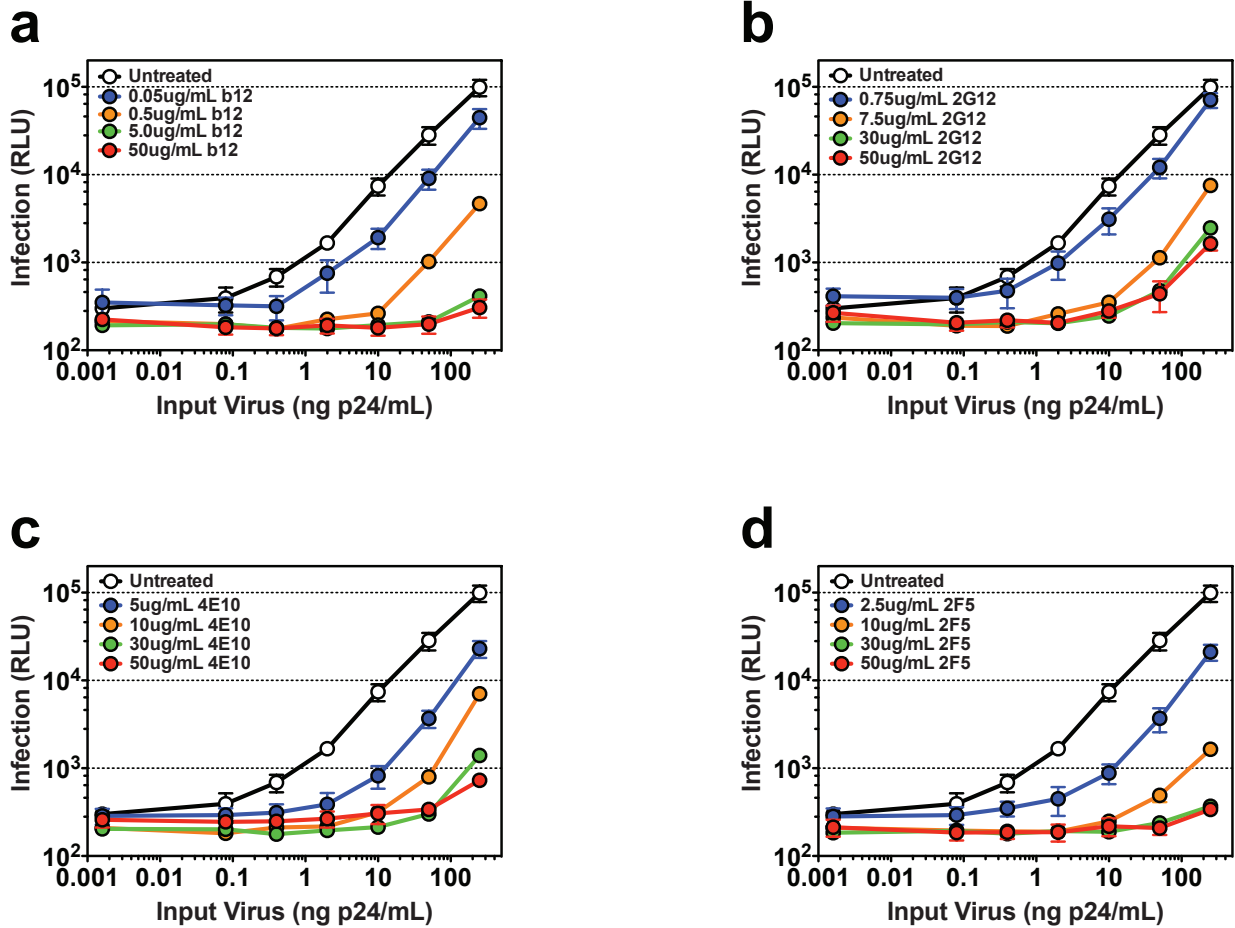
Supplementary Figure 2 – Map of the modular pVIP vector

Schematic representation of the pVIP transfer vector with unique restriction sites flanking each modular element designated in red. AAV sequences begin immediately following the XhoI restriction site with a 145bp “flip”-ITR from AAV2 followed by a SpeI restriction site and the immediate early CMV promoter. The promoter is followed by a NotI restriction site and one additional C residue to mimic a Kozak consensus sequence prior to the ATG of the luciferase transgene. The 3' end of the transgene is terminated with a TAA stop codon followed by one additional A residue prior to the BamHI site. The WPRE element follows this restriction site and continues until an Acc65I restriction site that precedes an SV40 polyadenylation signal and HindIII restriction site. Finally, a second 145bp AAV2 “flop”-ITR is located prior to an NheI site.



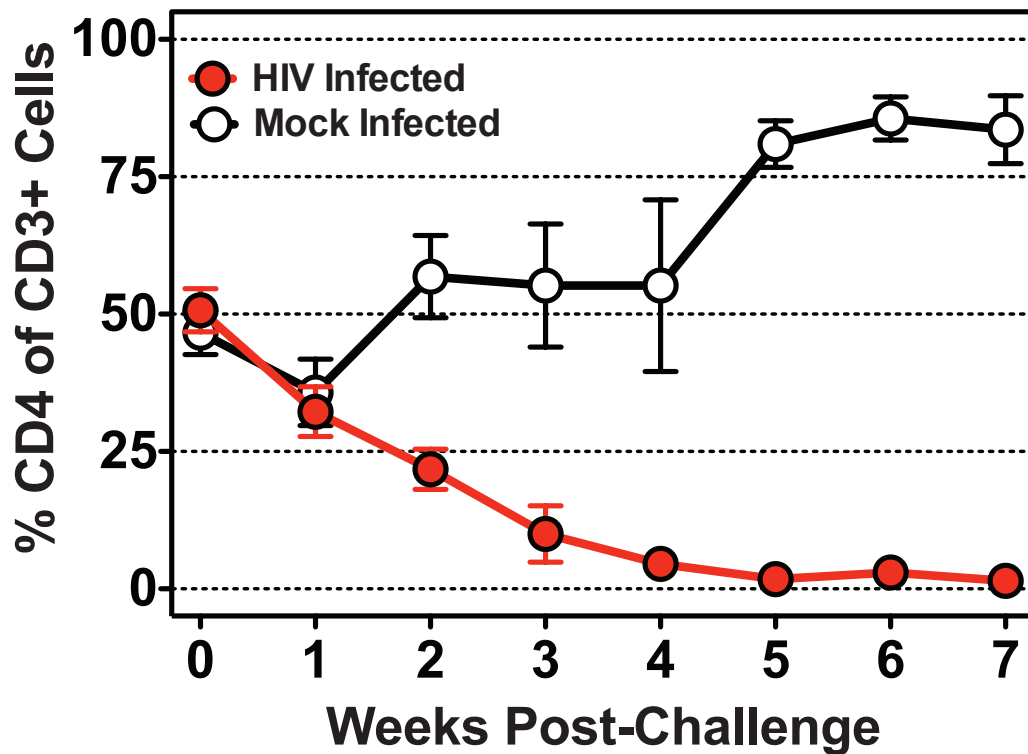
Supplementary Figure 3 – Optimization of the IgG1 transgene in vitro

a, Schematic representation of the IgG1 transgene that was optimized for expression in vitro. Highlighted are the heavy and light chain signal sequences (blue) the F2A self-processing peptide (green) and the predicted splice donor and acceptor sites (red lines). **b**, Comparison of antibody expression in vitro by ELISA following transfection with vectors carrying the antibody transgene shown above with standard or optimized F2A sequences that include a furin cleavage site. **c**, Comparison of 4E10 antibody expression in vitro by ELISA following transfection with vectors carrying 4E10 with natural or human growth hormone (HGH) derived signal peptides fused to the heavy chain gene, the light chain gene or both genes. **d**, Comparison of 4E10 antibody expression in vitro by ELISA following transfection with vectors carrying 4E10 in the standard expression cassette or a cassette in which the splice donors and acceptors were mutated to reduce the potential for extraneous splicing.



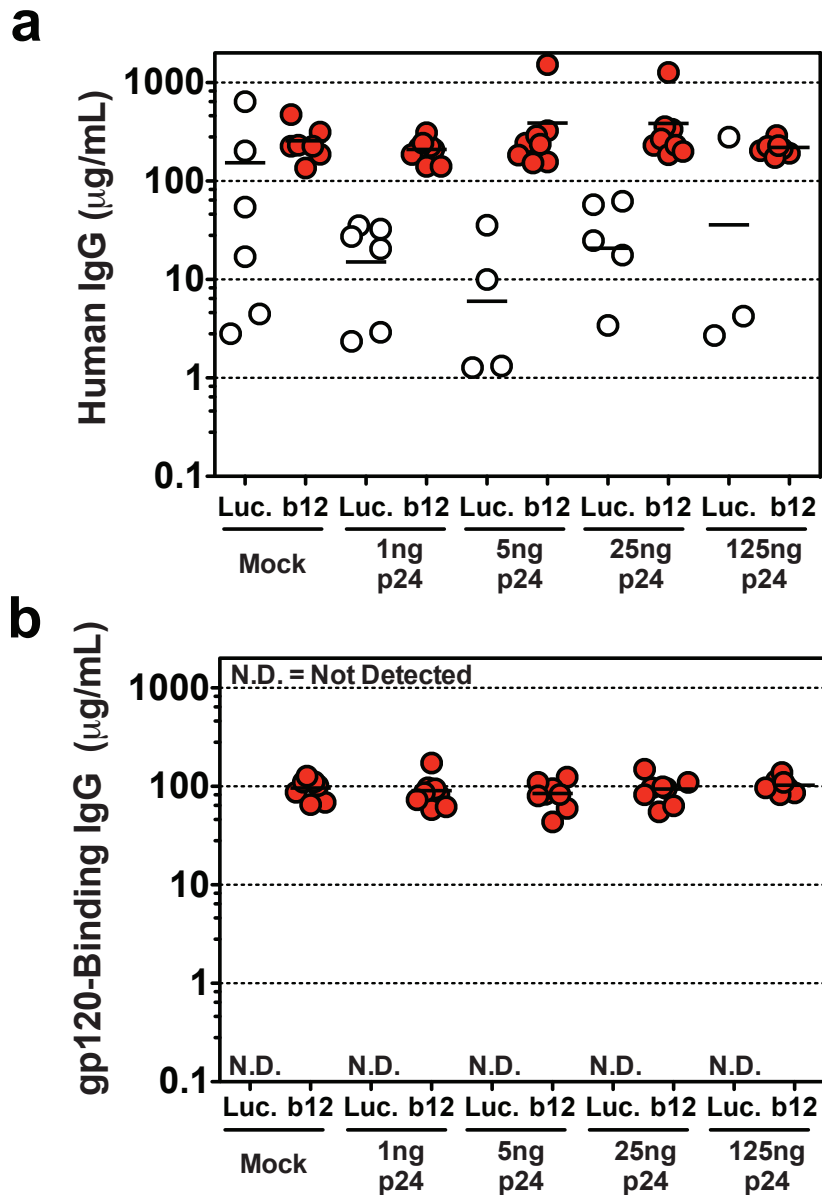
Supplementary Figure 4 – Neutralization of HIV by Antibodies expressed from an optimized expression transgene

To confirm that antibodies expressed from the optimized expression transgene retained their function, an in vitro protection assay using TZM-bl luciferase reporter cells was conducted. Cells were plated with the indicated concentrations of b12 (a), 2G12 (b), 4E10 (c) or 2F5 (d) prior to challenge with increasing titers of NL4-3. Two days after challenge, cells were lysed and quantitated for luciferase activity following the addition of luciferin substrate. (n=3, RLU=Relative luciferase Units).



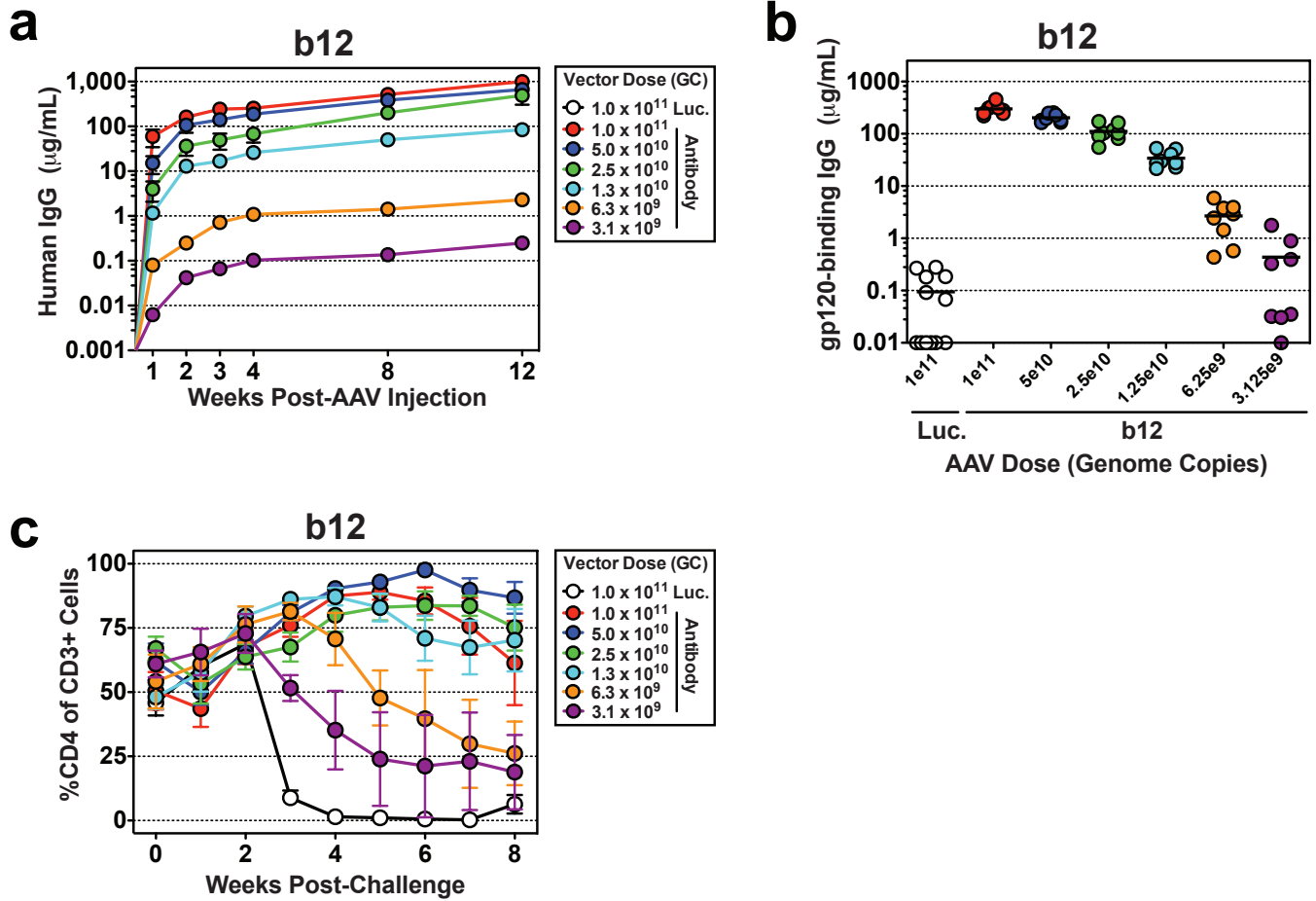
Supplementary Figure 5 – Depletion of CD4 cells in vivo following HIV challenge of humanized mice

Depletion of CD4+ T-cells in HuPBMC-NSG humanized mice following intraperitoneal (IP) challenge with 20ng p24 NL4-3 (n=4). To confirm that antibodies expressed from the optimized expression transgene retained their function, an in vitro protection assay using TZM-bl luciferase reporter cells was conducted. Cells were plated with the indicated concentrations of b12 (a), 2G12 (b), 4E10 (c) or 2F5 (d) prior to challenge with increasing titers of NL4-3. Two days after challenge, cells were lysed and quantitated for luciferase activity following the addition of luciferin substrate. (n=3, RLU=Relative luciferase Units).



Supplementary Figure 6 – Serum concentrations of total human IgG and gp120 binding IgG prior to HIV challenge

a, Concentration of total human antibody produced by engrafted cells and VIP as measured by human IgG ELISA on serum samples taken 5 weeks after intramuscular injection of vectors expressing either luciferase or b12 antibody and 3 weeks after adoptive transfer of human PBMCs and the day prior to IV HIV challenge (n=8). **b**, Concentration of antibody at the same time point quantified using a gp120-specific ELISA to measure the concentration of antibody specific for HIV (n=8).



Supplementary Figure 7 – Determination of the minimum protective dose of b12 *in vivo*

a, b12 expression over time as a function of dose as determined by total human IgG ELISA on serum samples taken following AAV administration (n=8). Mice receiving luciferase-expressing vector exhibited no detectable human antibodies (n=12). **b**, Concentration of b12 in serum one day prior to challenge, 3 weeks after adoptive transfer of human PBMCs and 15 weeks after intramuscular administration of the indicated dose of AAV as determined by a gp120-specific ELISA to measure the fraction of antibodies capable of binding HIV (n=8-12). **c**, CD4 cell depletion in HuPBMC-NSG humanized mice as a result of intravenous challenge with 10ng of NL4-3 into animals expressing a range of b12 demonstrating the minimum dose of antibody necessary to protect against infection. Plots **a** and **c** show mean and standard error, plot **b** shows individual animals and mean (n=8-12).

Supplementary Results

Optimal vectors for muscle-based antibody expression

To rapidly test novel vector configurations, we created a modular AAV transfer vector that implemented unique restriction sites flanking each modular element (Supplementary Fig. 2). To identify active promoters ideally suited to muscle expression, we created a series of vectors carrying the luciferase gene driven by a panel of ubiquitous and tissue-specific promoters. These vectors were administered intramuscularly via a single injection in the gastrocnemius muscle and luciferase expression was monitored to determine the relative expression potential of each promoter in this target tissue (Supplementary Fig. 1b). We identified the cytomegalovirus immediate early promoter (CMV), chimeric chicken- β -actin (CAG), and ubiquitin C (UBC) promoters as optimal for long-term muscle expression. Based on these findings, we created a novel promoter that combined these three promoters along with consensus splice donor and acceptor sequences to produce the CASI promoter design (Supplementary Fig. 1c). Further *in vivo* testing demonstrated that the CASI promoter was considerably more active in muscle than the CAG promoter despite being 34% more compact (Supplementary Fig. 1d). This reduced size allowed us to incorporate the woodchuck hepatitis virus posttranscriptional regulatory element (WPRE)³⁹, which we confirmed to significantly enhance expression of transgenes (Supplementary Fig. 1e). To determine the relative efficiency of polyadenylation signals for muscle-derived expression, we tested the SV40 late poly(A), the rabbit beta-globin (RBG) poly(A) and the bovine growth hormone (BGH) poly(A), all of which demonstrated comparable levels of expression (Supplementary Fig. 1e). Based on these results, we designed a muscle-optimized expression vector encoding an IgG1 scaffold into which heavy and light chain V-regions derived from monoclonal antibodies could be inserted (Supplementary Fig. 1f).

Optimization of the antibody transgene

To create an optimal framework for the expression of antibody, we cloned the heavy and light chains of several broadly neutralizing HIV antibodies separated by an F2A self-processing peptide sequence⁴⁰ (Supplementary Fig. 3a) into a mammalian expression vector under the control of the CMV promoter. 293T cells transfected with these vectors demonstrated secretion of human IgG into the culture supernatant that could be detected by ELISA (Supplementary Fig. 3b). In an attempt to improve expression, we re-engineered the F2A sequence to better reflect mammalian codon usage and incorporated a furin cleavage site at the N-terminus for optimal processing²². Comparison of these F2A optimized vectors by transfection showed they produced higher levels of all four antibodies tested.

We next sought to improve secretion of antibody by replacing the endogenous signal sequences with a codon optimized sequence derived from the well-characterized human growth hormone (HGH) and created versions of the 4E10 expression vector in which either the heavy chain, the light chain, or both chains were driven by separate HGH signal sequences and compared their expression by transfection. To minimize repetitive sequence in our viral vectors, two HGH sequences were synthesized which had distinct nucleotide sequences but encoded identical amino acids, and each were used for either the heavy or light chain exclusively. Replacement of the endogenous signal sequences with HGH sequences at either the heavy or light chains resulted in higher levels of antibody production, and signal sequence replacement of both chains yielded the best results (Supplementary Fig. 3c).

To remove the potential for inappropriate splicing of the transcript encoding the antibody, we subjected the sequence to *in silico* splice prediction⁴¹ and removed all potential splice donor

and acceptor sequences through the use of conservative mutations to the site or, when this was not possible, the surrounding sequences. We observed improved expression of the 4E10 antibody when placed in this splice-optimized framework (Supplementary Fig. 3d). The final antibody transgene consists of an HGH signal sequence followed by a swappable V_H region, a splice-optimized heavy chain constant region, a furin cleavage site linked to an optimized F2A peptide which is fused to a second HGH signal sequence, a swappable V_L region, and a splice-optimized kappa light chain constant region.

Validation of transgene-expressed antibody activity

To confirm that the optimizations made to improve gene expression did not impact the neutralizing efficacy of the antibodies, we expressed several well-studied broadly neutralizing antibodies from this expression cassette and tested these purified proteins in an *in vitro* protection assay. Cells carrying a luciferase gene under the control of HIV-induced transcriptional elements (TZM-bl cells) were incubated with dilutions of each antibody prior to challenge with increasing amounts of HIV. We observed robust reduction in TZM-bl cell infection at antibody concentrations that correlated well with the previously established IC₅₀ and IC₉₀ values for all antibodies tested against this strain (Supplementary Fig. 4).

Supplementary References

- 39 Zufferey, R., Donello, J. E., Trono, D. & Hope, T. J. Woodchuck hepatitis virus posttranscriptional regulatory element enhances expression of transgenes delivered by retroviral vectors. *J Virol* **73**, 2886-2892 (1999).
- 40 Szymczak, A. L. *et al.* Correction of multi-gene deficiency in vivo using a single 'self-cleaving' 2A peptide-based retroviral vector. *Nat Biotechnol* **22**, 589-594, doi:10.1038/nbt957 (2004).
- 41 Reese, M. G., Eeckman, F. H., Kulp, D. & Haussler, D. Improved splice site detection in Genie. *Journal of computational biology : a journal of computational molecular cell biology* **4**, 311-323 (1997).